

2015

## Altered Connexin 43 Expression Underlies Age-Dependent Decrease of Regulatory T Cell Suppressor Function in Nonobese Diabetic Mice

Michel Kuczma

Cong-Yi Wang

Leszek Ignatowicz

Robert Gourdi

Piotr Kraj

Old Dominion University, pkraj@odu.edu

Follow this and additional works at: [https://digitalcommons.odu.edu/biology\\_fac\\_pubs](https://digitalcommons.odu.edu/biology_fac_pubs)



Part of the [Cell Biology Commons](#), [Immunology and Infectious Disease Commons](#), and the [Molecular Biology Commons](#)

---

### Original Publication Citation

Kuczma, M., Wang, C. Y., Ignatowicz, L., Gourdie, R., & Kraj, P. (2015). Altered connexin 43 expression underlies age-dependent decrease of regulatory T cell suppressor function in nonobese diabetic mice. *Journal of Immunology*, 194(11), 5261-5271. doi:10.4049/jimmunol.1400887

This Article is brought to you for free and open access by the Biological Sciences at ODU Digital Commons. It has been accepted for inclusion in Biological Sciences Faculty Publications by an authorized administrator of ODU Digital Commons. For more information, please contact [digitalcommons@odu.edu](mailto:digitalcommons@odu.edu).

# Altered Connexin 43 Expression Underlies Age-Dependent Decrease of Regulatory T Cell Suppressor Function in Nonobese Diabetic Mice

Michal Kuczma,\* Cong-Yi Wang,\*<sup>†</sup> Leszek Ignatowicz,\* Robert Gourdie,<sup>‡</sup> and Piotr Kraj\*

Type 1 diabetes is one of the most extensively studied autoimmune diseases, but the cellular and molecular mechanisms leading to T cell–mediated destruction of insulin-producing  $\beta$  cells are still not well understood. In this study, we show that regulatory T cells ( $T_{\text{regs}}$ ) in NOD mice undergo age-dependent loss of suppressor functions exacerbated by the decreased ability of activated effector T cells to upregulate Foxp3 and generate  $T_{\text{regs}}$  in the peripheral organs. This age-dependent loss is associated with reduced intercellular communication mediated by gap junctions, which is caused by impaired upregulation and decreased expression of connexin 43. Regulatory functions can be corrected, even in T cells isolated from aged, diabetic mice, by a synergistic activity of retinoic acid, TGF- $\beta$ , and IL-2, which enhance connexin 43 and Foxp3 expression in  $T_{\text{regs}}$  and restore the ability of conventional CD4<sup>+</sup> T cells to upregulate Foxp3 and generate peripherally derived  $T_{\text{regs}}$ . Moreover, we demonstrate that suppression mediated by  $T_{\text{regs}}$  from diabetic mice is enhanced by a novel reagent, which facilitates gap junction aggregation. In summary, our report identifies gap junction–mediated intercellular communication as an important component of the  $T_{\text{reg}}$  suppression mechanism compromised in NOD mice and suggests how  $T_{\text{reg}}$  mediated immune regulation can be improved. *The Journal of Immunology*, 2015, 194: 5261–5271.

Type 1 diabetes (T1D) is a complex autoimmune disease resulting from destruction of pancreatic  $\beta$ -islets by infiltrating immune cells (1). Both environmental and genetic factors contribute to the development of the disease in humans and in NOD mice, which constitute an animal model of diabetes (2). Cellular mechanisms implicated in the progression of T1D include aberrant activation of autoreactive T cells, inefficient peripheral tolerance, and impaired function of immunoregulatory cells, especially CD4<sup>+</sup> regulatory T cells ( $T_{\text{regs}}$ ) expressing the transcription factor Foxp3 (1, 3).

$T_{\text{regs}}$  regulate homeostasis of the immune system and a variety of immune responses, including autoimmunity, and rely on numerous mechanisms that involve soluble, immunomodulatory cytokines, IL-10 and TGF- $\beta$ , as well as membrane molecules and cell contact–dependent interactions (4, 5).  $T_{\text{regs}}$  may also sustain tolerance by converting effector CD4<sup>+</sup> T cells into  $T_{\text{regs}}$ . This mechanism of “infectious” tolerance relies on genetic reprogramming of effector cells to become  $T_{\text{regs}}$  and involves intercellular transport of cAMP (6, 7). The determinants of which

suppression mechanisms are used in particular immune contexts remain poorly understood.

Two major subsets of  $T_{\text{regs}}$ , thymus-derived ( $tT_{\text{reg}}$ ) and peripherally derived  $T_{\text{regs}}$  ( $pT_{\text{reg}}$ ), were defined based on whether their suppressor function is acquired during normal thymic T cell development or after antigenic stimulation in peripheral lymphoid organs (8). In vitro–induced  $T_{\text{regs}}$  ( $iT_{\text{reg}}$ ) may be generated by stimulation of CD4<sup>+</sup> T cells in the presence of TGF- $\beta$  and IL-2 (5). In vivo  $pT_{\text{regs}}$  are induced by a specialized population of dendritic cells in a process dependent on TGF- $\beta$  and retinoic acid (RA) (9). Treatment of NOD mice with RA delayed the development of diabetes by inducing and expanding  $T_{\text{regs}}$ , and by protecting islets from immune system–mediated destruction (10, 11).

Several lines of evidence directly showed that  $T_{\text{regs}}$  regulate autoimmunity in diabetes. Transfer of  $pT_{\text{regs}}$  or  $iT_{\text{regs}}$  into NOD mice, or in vivo induction of  $T_{\text{regs}}$ , can protect NOD mice from diabetes (12–14). Conversely, compromised function of  $T_{\text{regs}}$  was found to induce or exacerbate diabetes (15, 16). A number of genes associated with diabetes susceptibility loci regulate the survival and/or functions of  $T_{\text{regs}}$  (e.g., CTLA4, IL-2, STAT5) (17–19). Despite clear evidence of  $T_{\text{reg}}$  influence on T1D development, it remains controversial as to what the changes are in the  $T_{\text{reg}}$  population that actually contribute to the natural pathogenesis of diabetes in NOD mice. Although some studies suggested a primary defect in the number and/or suppressor function of  $T_{\text{regs}}$ , other studies pointed to the resistance of effector T cells to  $T_{\text{reg}}$ –mediated suppression as a possible mechanism of autoimmune diabetes (20–25). Some of the discrepancies in the experimental results may stem from the use of different markers (e.g., CD25 or Foxp3), to identify and isolate the  $T_{\text{reg}}$  population.

To better define the cellular and molecular basis of impaired  $T_{\text{reg}}$  function in diabetes, we examined populations of these cells in young, prediabetic and aged, diabetic NOD mice expressing a Foxp3<sup>GFP</sup> reporter that allows for unambiguous identification of  $T_{\text{regs}}$ . We have found that compromised suppression mediated by

\*Center for Biotechnology and Genomic Medicine, Georgia Regents University, Augusta, GA 30912; <sup>†</sup>The Center for Biomedical Research, Tongji Hospital, Tongji Medical College, Huazhong University of Science and Technology, Wuhan, 430030, China; and <sup>‡</sup>Virginia Tech Carilion Research Institute, Roanoke, VA 24015

Received for publication April 4, 2014. Accepted for publication March 24, 2015.

This work was supported by the Juvenile Diabetes Research Foundation (Award 5-20080321) and National Cancer Institute Grant R01 CA151550 (to P.K.).

Address correspondence and reprint requests to Dr. Piotr Kraj at the current address: Department of Biological Sciences, Old Dominion University, Mills Goodwin Building, 5115 Hampton Boulevard, Norfolk, VA 23529. E-mail address: pkraj@odu.edu

The online version of this article contains supplemental material.

Abbreviations used in this article: Cx43, connexin 43;  $iT_{\text{reg}}$ , induced  $T_{\text{reg}}$ ; LN, lymph node;  $pT_{\text{reg}}$ , peripherally derived  $T_{\text{reg}}$ ; RA, retinoic acid; T1D, type 1 diabetes;  $T_{\text{reg}}$ , regulatory T cell;  $tT_{\text{reg}}$ , thymus-derived  $T_{\text{reg}}$ ; ZO-1, zona occludens-1.

Copyright © 2015 by The American Association of Immunologists, Inc. 0022-1767/15/\$25.00

T<sub>regs</sub> was associated with decreased ability of conventional T cells to upregulate Foxp3 and convert into iT<sub>regs</sub> in aging NOD mice. We show that expression of connexin 43 (Cx43), a gap junction protein and one of the TGF- $\beta$ -inducible genes, progressively declined in NOD mice progressing to diabetes. Gap junctions are essential for transporting cAMP from T<sub>regs</sub> into target T cells, which initiates the genetic program of inhibiting T cell activation (7, 26). In this study, we found that dysregulated expression of Cx43 and alleviated cAMP signaling underlie progressive loss of T<sub>reg</sub> suppressor function in NOD mice. This signaling defect and impaired iT<sub>reg</sub> generation can be corrected by treatment of effector T cells with TGF- $\beta$ , which promotes upregulation of Cx43, and RA, which regulates phosphorylation of connexin molecules and intercellular communication through gap junctions. Our data suggest that interactions that require cell contact and intercellular communication are compromised in aged T cells in NOD mice. Finally, using a novel reagent that inhibits a PDZ-based interaction of Cx43 with the scaffolding protein zona occludens-1 (ZO-1), we demonstrate that suppressor function could be augmented even in T<sub>regs</sub> isolated from NOD mice with diabetes.

## Materials and Methods

### Mice

NOD mice expressing Foxp3<sup>GFP</sup> reporter (NOD<sup>GFP</sup> mice) were constructed as reported previously (27). A fragment of Foxp3 locus (located on BAC clone RP23-446O15) was modified to express GFP controlled by the Foxp3 regulatory sequences. Transgenic mice were produced in Joslin Diabetes Center at Harvard University by injecting NOD oocytes. Founders were identified by PCR of tail DNA.

All control mice were healthy, 2- to 4-wk-old NOD<sup>GFP</sup> prediabetic females referred to in this text as young mice, and diseased animals, referred to as diabetic, were  $\geq$ 20-wk-old females with diabetes (mice with blood glucose levels  $<$ 120 mg/dl were considered healthy and those with levels  $>$ 300 mg/dl were considered diabetic). In some experiments, age-matched Foxp3<sup>GFP</sup> reporter mice on the C57BL/6 (C57BL/6-Tg [Foxp3-GFP]90Pkraj/J; Jackson Labs) genetic background (B6<sup>GFP</sup> mice) were used as additional controls. The incidence rate of diabetes in our colony was observed to be 85–90% for females and 15–20% for males.

Diabetes was induced in 5- to 6-mo-old female B6<sup>GFP</sup> mice by streptozotocin injections. Streptozotocin (Sigma-Aldrich) was dissolved in 0.1 M citrate buffer (pH 4.5) and injected i.p. at a dose of 50 mg/kg/d for 5 d (28). Mice were sacrificed at day 14 after initial injection when blood glucose levels, measured for three consecutive days, were  $>$ 350 mg/dl.

Full details of the study and all procedures performed on animals were approved by the Institutional Animal Care and Use Committee of the Georgia Regents University (approval #09-06-213) and complied with all state, federal, and National Institutes of Health regulations.

### Cell purification, flow-cytometry analysis, and cell sorting

Cells from peripheral (axillary, brachial, and inguinal), mesenteric, and pancreatic lymph node (LN), spleens, and thymi were stained with Abs specific for CD4, CD8, CD25, CD44, CD62L, CTLA4, GITR, pSTAT5, Helios, and anti-rat CD2 (rCD2; BD, eBioscience, Biolegend), and analyzed on a BD FACSCanto instrument. Cells were sorted on a MoFlo cell sorter (Beckman Coulter; purity of all sorts exceeded 98%). Data were analyzed using FlowJo (Tree Star).

### Detection of p-STAT5

p-STAT5 was detected in CD4<sup>+</sup> T cells isolated from pancreatic LNs from young and old NOD<sup>GFP</sup> mice and from B6<sup>GFP</sup> mice by intracellular staining as described previously (29). LN cells were cultured in complete media in the presence of IL-2 (10 ng/ml), stained with Abs specific for CD4, CD8, and CD25, washed, fixed, and stained with p-STAT5 Ab (pY694; BD).

### Induction of Foxp3 expression

Sorted CD4<sup>+</sup>Foxp3<sup>GFP</sup> cells were activated with plate-bound anti-CD3 (10  $\mu$ g/ml) and anti-CD28 (1  $\mu$ g/ml) Abs (Biolegend) in the presence of recombinant murine IL-2 (50 U/ml) and TGF- $\beta$  (3 ng/ml) (both from

Proteotech) and monitored daily for GFP and Foxp3 upregulation by flow cytometry and RT-PCR. Some wells contained RA (3 nM; Sigma-Aldrich). This experiment was done at least five times.

### RT-PCR

Total RNA was isolated using the RNeasy Mini Kit (Qiagen) and converted into cDNA using the Superscript III kit (Invitrogen). Gene expression studies were performed using quantitative real-time PCR and TaqMan probes (Invitrogen). All data were normalized for  $\beta$ -actin expression, and expression differences were shown as relative expression. Data were acquired with ABI7900HT instrument. All primers had been used previously (27, 30).

Analysis of Foxp3 expression in single cells was done as described previously. In brief, single cells were sorted from populations of CD4<sup>+</sup>Foxp3<sup>GFP</sup> and T<sub>regs</sub> expressing low and high levels of Foxp3 directly into 96-well PCR plates containing reverse transcription buffer, and cDNA was synthesized. Foxp3 and  $\beta$ -actin transcripts were amplified by two rounds of PCR using nested primers: Foxp3: first round 5'-GCCTGCCACCTGGGATCAAT-3' and 5'-CACAGATGGAGCCTGGCCA-3' primers, second round 5'-CACCCAGGAAAGACAGCAACC-3' and 5'-CTTCTCTTTCCAGCTCCAGC-3';  $\beta$ -actin: first round 5'-GACATG-GAGAAAGATCTGGACCA-3' and 5'-CTCTTTGATGTCACGCACGATT-TC-3' and second round 5'-CCTTCTACAATGAGCTGCGTGTGGC-3' and 5'-CATGAGGTAGTCTGTCAAGTCC-3' primers (30, 31).

### Western blot

Sorted CD4<sup>+</sup>GFP<sup>-</sup>, CD4<sup>+</sup>GFP<sup>+</sup>, or CD4<sup>+</sup>CD25<sup>-</sup>, CD4<sup>+</sup>CD25<sup>+</sup> cells were lysed directly in SDS-loading buffer and resolved on 12% polyacrylamide gel ( $5 \times 10^4$  cells/lane) and electrotransferred onto a PVDF membrane (Millipore). Membranes were probed with Ab specific for Foxp3 (1  $\mu$ g/ml, eBio7979; eBioscience) as described previously (27). For Smad2 and phospho-Smad2 detection, membranes were probed overnight (4°C) with the corresponding Abs (Cell Signaling Technology). Images were scanned and analyzed using ImageQuant 5.2 software (GE).

### Proliferation inhibition assay

Sorted CD4<sup>+</sup>Foxp3<sup>GFP</sup> cells were used as T<sub>regs</sub> and CD4<sup>+</sup>Foxp3<sup>GFP</sup> cells as responders as described previously (27). Responder cells ( $5 \times 10^4$ /well) were incubated on a 96-well plate with irradiated splenocytes ( $5 \times 10^4$ /well, 3000 rad) and soluble anti-CD3 $\epsilon$  Ab (5  $\mu$ g/ml). Various numbers of sorted CD4<sup>+</sup>Foxp3<sup>GFP</sup> cells ( $0.25$ – $5 \times 10^4$ /well) were added. Cells were sorted using MoFlo sorter. Proliferation was assessed by measurement of incorporated [<sup>3</sup>H]thymidine added (1  $\mu$ Ci/well) on the third day of a 4-d culture. For some assays, Gap26 (100  $\mu$ M; Anaspec) or  $\alpha$ CT-1 (75  $\mu$ M; American Peptide Company) peptides were added to the wells.

### Measurement of IFN- $\gamma$

Flow-cytometry-sorted CD4<sup>+</sup>Foxp3<sup>GFP</sup> effector cells were mixed with increasing proportions of sorted CD4<sup>+</sup>Foxp3<sup>GFP</sup> T<sub>regs</sub> and irradiated splenocytes, and stimulated with soluble anti-CD3 $\epsilon$  Ab as described earlier. Levels of IFN- $\gamma$  in the culture supernatant were measured in triplicates with commercial ELISA kit (eBioscience).

### STAT5b and Cx43 overexpression

Full-length cDNA encoding a constitutively active form of STAT5b (STAT5b-CA; gift of Dr. A. Farrar, University of Minnesota) or Cx43 (Open Biosystems) were cloned into retroviral vector pMx-IRES-rCD2 expressing extracellular rat CD2 domain (gift of Dr. M. Iwashima, Loyola University). Retroviral particles were prepared in Phoenix-Eco packaging cell line (gift of Dr. G. Nolan, Stanford University), and culture media were used to infect target cells. Sorted CD4<sup>+</sup>Foxp3<sup>GFP</sup> cells ( $5$ – $10 \times 10^4$ ) were activated with anti-CD3 and anti-CD28 Abs and spin-infected with viral supernatant. Transduction efficiency was assessed by staining for rat CD2 extracellular domain. Transduced cells in some wells were incubated with IL-2/TGF- $\beta$  or RA.

For retroviral transduction of T<sub>regs</sub>, sorted Foxp3<sup>GFP</sup> cells were activated overnight as described earlier in the presence of IL-2 (50 U/ml). Cells were then infected with Cx43-encoding or control virus and further expanded on anti-CD3/anti-CD28-coated plates in the presence of IL-2. Two days later, rCD2 expression was assessed by flow cytometry. T<sub>regs</sub> expressing a high level of rCD2 ( $>$ 90%) were used as suppressors, and freshly sorted CD4<sup>+</sup>Foxp3<sup>GFP</sup> cells were used as effector cells in proliferation inhibition assay.

### Calcein loading and dye transfer

iT<sub>regs</sub> and activated T cells were prepared from CD4<sup>+</sup> T cells expressing transgenic TCR specific for pigeon cytochrome *c* antigenic peptide presented by I-A<sup>b</sup> (32). iT<sub>regs</sub> were loaded with 0.5 μM calcein violet, AM (Invitrogen) according to manufacturer's instructions and stained with anti-CD4-allophycocyanin. Responder cells stained with anti-CD4-PE were mixed with iT<sub>regs</sub> and bone marrow-derived dendritic cells at 1:1:0.1 ratio in the presence (0.25 μM) or absence of antigenic peptide. Cells were seeded in a round-bottom 96-well plate, and calcein transfer into responder CD4-PE cells was recorded after 5 h using LSRII flow cytometer (BD) equipped with violet laser.

### Statistical analysis

All data are presented as the mean values ± SD. The significance of differences between samples or groups of mice was determined using paired, one-tailed Student *t* test. Differences between samples with *p* values ≤0.05 were considered significant. Statistical analysis was done using Origin 9.0 software (OriginLab).

## Results

### The suppressor function but not cell numbers of T<sub>regs</sub> decline in aged NOD mice

To uncover what cellular and molecular characteristics are associated with progression to disease, we have studied phenotypes and an abundance of CD4<sup>+</sup> T cell subsets in peripheral and pancreatic LNs of young (2–4 wk) NOD mice with normal glucose levels (120 mg/dl) and diabetic NOD mice (≥20 wk) with overt diabetes (>300 mg/dl glucose). To facilitate identification of T<sub>regs</sub>, we have produced Foxp3<sup>GFP</sup> reporter mice (NOD<sup>GFP</sup>). A modified BAC clone previously used to generate Foxp3<sup>GFP</sup> reporter mice in the C57BL/6 strain (B6<sup>GFP</sup>) was introduced into NOD oocytes (Fig. 1A–D) (27). Thus, the generation of our reporter mice did not involve backcrossing of transgenic founder animals onto an NOD genetic background. Transgenic reporter and wild type NOD mice had equivalent numbers, percentages, and cell-surface phenotypes of all T cell subsets, including CD4<sup>+</sup>CD25<sup>+</sup> T cells, in thymus, LNs, and spleen. Consistent with earlier reports, a normal, or even increased, proportion of Foxp3<sup>GFP+</sup> T cells was observed in NOD<sup>GFP</sup> mice of every age, including young and diabetic mice (Fig. 1E, 1F) (24). Moreover, we observed a moderate increase of T<sub>regs</sub> in peripheral and pancreatic LNs. Despite stable proportions of T<sub>regs</sub>, we observed phenotypic changes of T<sub>reg</sub> populations: cells from diabetic mice expressed lower levels of GITR, CTLA4, and Helios, but higher levels of CD39 and PD-1 (Fig. 1G and data not shown). Aged NOD<sup>GFP</sup> mice had expanded populations of activated CD44<sup>+</sup>CD62L<sup>-</sup> conventional CD4<sup>+</sup> T cells in peripheral LNs including pancreatic LNs (Fig. 1H, 1I). We have also observed enhanced proliferative responses of Foxp3<sup>GFP-</sup> effector cells stimulated in vitro, which correlated with increased blood glucose levels (Fig. 1J, 1K).

Because disease progression was not associated with declining proportions of T<sub>regs</sub>, we checked the ability of these cells to suppress the immune response. For that purpose, we examined T<sub>regs</sub> expressing low and high levels of Foxp3 from young and diabetic NOD<sup>GFP</sup> mice in a standard proliferation inhibition assay and compared these mice with diabetes-resistant B6<sup>GFP</sup> mice. We consistently observed decreased capacity of T<sub>regs</sub> isolated from diabetic animals to inhibit proliferation of activated, conventional (CD4<sup>+</sup>Foxp3<sup>GFP-</sup>) Th cells from young NOD<sup>GFP</sup> mice (Fig. 2A). However, T<sub>regs</sub> from both young and diabetic NOD<sup>GFP</sup> mice had lower suppressor capacity than corresponding cells from B6<sup>GFP</sup> mice. In a reciprocal experiment, T<sub>regs</sub> from young NOD<sup>GFP</sup> mice were able to significantly inhibit proliferation of effector CD4<sup>+</sup> T cells from older, diabetic animals. Finally, proliferation inhibition was smallest when T<sub>regs</sub> and responder cells were both iso-

lated from aged, diabetic mice (Fig. 2B). To examine whether hyperglycemia could alter T<sub>reg</sub> functions, we have induced diabetes in 4- to 5-mo-old B6 mice by streptozotocin injection. This experiment shows comparable inhibition of proliferation and IFN-γ production by cells isolated from normal and hyperglycemic mice, demonstrating that observed differences in T<sub>reg</sub> suppression are likely not caused by differences in blood glucose levels (Supplemental Fig. 1A, 1B). Together, our data demonstrate that functional, not quantitative, changes of T<sub>regs</sub> are associated with disease progression in NOD mice. Higher proportion of T<sub>regs</sub> from old NOD mice than from young and aged B6 mice is needed to achieve the same level of suppression, suggesting that immune environment permissive for autoimmune disease already exists before overt diabetes.

### Effector CD4<sup>+</sup> T cells and Foxp3<sup>GFPlo</sup> T<sub>regs</sub> from diabetic mice have decreased ability to upregulate Foxp3 expression when activated in the presence of IL-2 and TGF-β

We have routinely observed that a small, but consistent proportion of sorted naive CD4<sup>+</sup> T cells from B6<sup>GFP</sup> mice upregulated Foxp3 when activated in vitro without exogenous IL-2 and TGF-β (30). In NOD mice, we noticed that a larger fraction of effector cells from young NOD<sup>GFP</sup> mice than from older mice upregulated Foxp3 when cells were activated in vitro (Fig. 3A). This age-dependent decline in the ability of effector T cells to upregulate Foxp3, not seen in aging B6<sup>GFP</sup> mice, suggests reduced and delayed capacity to generate iT<sub>regs</sub> in aged NOD mice (Fig. 3B).

Consistent with our previous analysis of B6<sup>GFP</sup> reporter mice, we examined whether the population of T<sub>regs</sub> in NOD<sup>GFP</sup> mice is heterogeneous, with cells being differentially sensitive to Ag/cytokine stimulation. To examine how Foxp3 is regulated in T cell subsets in young and aged NOD<sup>GFP</sup> mice, we activated conventional CD4<sup>+</sup>Foxp3<sup>-</sup> cells and Foxp3<sup>lo</sup> and Foxp3<sup>hi</sup> T<sub>regs</sub> with plate-bound anti-CD3/anti-CD28 Abs without and in the presence of TGF-β and IL-2 (33). A large proportion of Foxp3<sup>hi</sup> T<sub>regs</sub>, which constituted a majority of the T<sub>reg</sub> population, preserved a stable T<sub>reg</sub> phenotype in young and old NOD<sup>GFP</sup> mice when activated (Fig. 3C, 3D). In contrast, conventional Foxp3<sup>-</sup> cells and Foxp3<sup>lo</sup> T<sub>regs</sub> from aged NOD<sup>GFP</sup> mice have a decreased ability to upregulate and/or maintain Foxp3 expression compared with the respective populations from young mice. In particular, the Foxp3<sup>lo</sup> subset in aged mice had an unstable T<sub>reg</sub> phenotype, and only a small proportion of these cells was able to sustain Foxp3 expression when stimulated with anti-CD3/anti-CD28 Abs even in the presence of TGF-β (Fig. 3D). Altogether, our results suggest that CD4<sup>+</sup> T cell populations, identified in previous reports as precursors of pT<sub>regs</sub>, are most affected by the dysregulated expression of Foxp3 in aging NOD mice.

### Dysregulated upregulation/expression of Foxp3 in aged NOD mice is associated with decreased signaling through STAT5 and Smad2/3

To delineate molecular mechanisms of age-related weakening of T<sub>reg</sub> suppression, we examined regulation of Foxp3 expression by IL-2 and TGF-β. IL-2 and TGF-β are cytokines critical for generation and maintenance of peripheral T<sub>regs</sub> (34). Previous studies have shown that components of the IL-2 signaling pathway map to diabetes susceptibility loci (19, 35, 36). Mutations of STAT5, a component of the IL-2R signaling pathway, were associated with impaired function of T<sub>regs</sub> in NOD mice (18). Similarly, TGF-β, acting through Smad2/3, was found to regulate genes controlling T<sub>reg</sub> functions and insulin-specific T<sub>regs</sub> (37, 38). Decreased expression and/or phosphorylation of STAT5 or Smad2/3 could suggest impaired signaling by IL-2 and TGF-β receptors, and



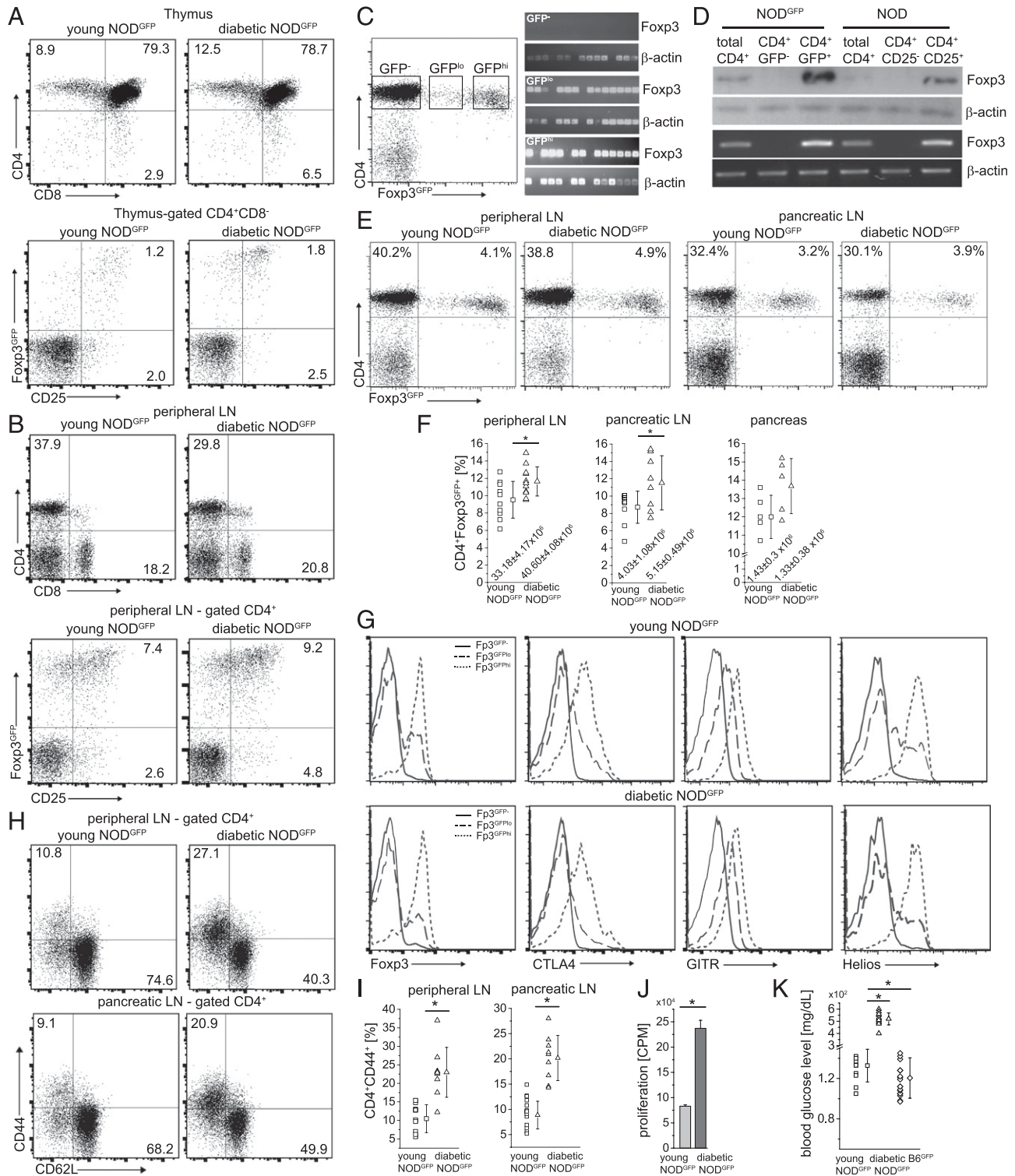


**FIGURE 1.** Analysis of T cell subsets in young and diabetic NOD mice expressing Foxp3<sup>GFP</sup> reporter transgene. **(A and B)** Flow-cytometry analysis of cells from thymus (A) and peripheral LN (B) of young and diabetic mice. Dot plots show expression of CD4 and CD8 on the populations of total thymic and LN cells (*upper panels*) and expression of CD25 and Foxp3<sup>GFP</sup> on gated CD4<sup>+</sup> cells (*lower panels*). **(C)** Analysis of Foxp3 expression in single cells expressing low and high levels of Foxp3 (*left panel* shows gating strategy used for cell sorting). Single cells were sorted onto 96-well plates, and β-actin amplification was used to identify wells containing cells. **(D)** The Foxp3<sup>GFP</sup> transgene is expressed exclusively in cells expressing endogenous Foxp3. Western blot (*upper panels*) and RT-PCR (*lower panels*) analysis of Foxp3 expression in total CD4<sup>+</sup> T cells and CD4<sup>+</sup>Foxp3<sup>GFP-</sup>, CD4<sup>+</sup>Foxp3<sup>GFP+</sup> subsets sorted from NOD<sup>GFP</sup> mice, and in total CD4<sup>+</sup> T cells and CD4<sup>+</sup>CD25<sup>-</sup> and CD4<sup>+</sup>CD25<sup>+</sup> subsets sorted from wild-type NOD mice. β-Actin was used to normalize samples. **(E)** Expression of CD4 and Foxp3 in peripheral and pancreatic LNs in young and diabetic NOD mice. **(F)** Proportions of Foxp3<sup>GFP+</sup> in populations of gated CD4<sup>+</sup> T cells isolated from peripheral and pancreatic LNs and pancreas of young and diabetic NOD mice. The absolute numbers of cells isolated from peripheral, pancreatic LNs and from pancreas are shown as plot inserts. Cells isolated from inguinal, brachial, and axillary LNs were combined for peripheral LN analysis. Individual young mice are represented by squares (□), and diabetic mice are represented by triangles (△). Mean values and standard deviations are shown by bars. **(G)** Expression of endogenous Foxp3, CTLA4, GITR, and Helios in sorted populations of Foxp3<sup>GFP-</sup> (solid line), Foxp3<sup>GFPlo</sup> (broken line), and Foxp3<sup>GFP+</sup> (dotted line) cells. **(H)** Percentage of activated CD44<sup>+</sup>CD62L<sup>-</sup> cells in the (Figure legend continues)

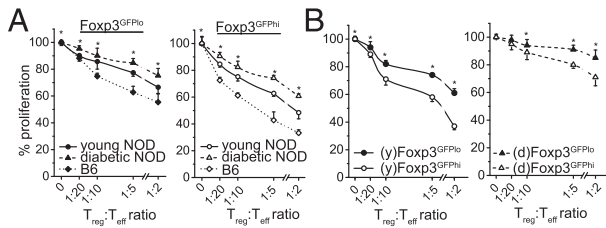


**FIGURE 2.**  $T_{reg}$ s from aged  $NOD^{GFP}$  mice lose suppressor function. **(A)** T cell proliferation inhibition assay with  $T_{reg}$ s sorted from young and diabetic  $NOD^{GFP}$  mice. Circles, triangles, and diamonds represent  $T_{reg}$ s from young and diabetic  $NOD^{GFP}$  and  $B6^{GFP}$  mice, respectively, expressing low ( $\bullet$ ,  $\blacktriangle$ ,  $\blacklozenge$ ) and high ( $\circ$ ,  $\triangle$ ,  $\lozenge$ ) levels of Foxp3. Gating strategy to isolate  $T_{reg}$ s expressing low and high levels of Foxp3 is shown in Fig. 1C.  $CD4^+$  Foxp3 $^{GFP-}$  responder cells were sorted from young  $NOD^{GFP}$  mice. Asterisks denote data points statistically different ( $*p < 0.05$ ) between young and aged  $NOD^{GFP}$  mice. One of at least three independent experiments is represented. **(B)** Conventional  $CD4^+$  Foxp3 $^{GFP-}$  cells from diabetic  $NOD^{GFP}$  mice remain sensitive to suppression by  $T_{reg}$ s from young  $NOD^{GFP}$  mice and to a much lower extent by  $T_{reg}$ s from diabetic mice. Proliferation of  $CD4^+$  Foxp3 $^{GFP-}$  responder cells sorted from diabetic  $NOD^{GFP}$  mice is inhibited by  $T_{reg}$ s expressing low ( $\bullet$ ,  $\blacktriangle$ ) or high levels of Foxp3 ( $\circ$ ,  $\triangle$ ) sorted from young (y) (*left panel*) and diabetic (d) (*right panel*)  $NOD^{GFP}$  mice. The experiment was repeated two times. Error bars denote mean  $\pm$  SD.  $*p < 0.05$ .

explain decreased  $T_{reg}$  suppression in aging NOD mice. To test this hypothesis, we studied protein expression- and signaling-induced phosphorylation of STAT5 or Smad2/3 in young and diabetic NOD mice.

As shown in Fig. 4A and 4C, T cells from peripheral and pancreatic LNs of young and diabetic  $NOD^{GFP}$  mice express similar levels of STAT5, but much lower levels of Smad2/3. When activated in the presence of IL-2 and TGF- $\beta$ , decreased levels of STAT5 and Smad2/3 phosphorylation were found in T cells from diabetic mice (Fig. 4B, 4D). When compared with  $B6^{GFP}$  mice, decreased STAT5 phosphorylation was found even in  $CD4^+$  T cells from young mice (Fig. 4B). A recent report demonstrated that mice with a constitutively active form of STAT5 have more  $T_{reg}$ s (39). To determine whether increased STAT5 signaling promotes Foxp3 upregulation, we transduced  $CD4^+$  T cells from  $NOD^{GFP}$  and  $B6^{GFP}$  mice with a retroviral vector expressing a constitutively active STAT5 mutant (gift of Dr. M. Farrar) and activated them in the presence of IL-2 and TGF- $\beta$  (40). Enhanced signaling mediated by STAT5 resulted in an increased proportion of cells upregulating Foxp3 only in effector cells isolated from  $B6^{GFP}$  mice (Supplemental Fig. 2). Collectively, examining STAT5 and Smad2/3 shows that impaired signaling by IL-2 and TGF- $\beta$  likely contributes to age-dependent decrease of  $T_{reg}$  functions in diabetic NOD mice.

#### Decreased expression/upregulation of Cx43 in old NOD mice underlies impaired suppressor function of $T_{reg}$ s

In an attempt to restore Foxp3 upregulation in T cells isolated from diabetic  $NOD^{GFP}$  mice to the levels observed in young  $NOD^{GFP}$  mice, we treated naive cells isolated from diabetic  $NOD^{GFP}$  mice

with RA. As shown in Fig. 5A, addition of RA to T cells activated in the presence of IL-2 and TGF- $\beta$  resulted in a significant increase in the proportion of  $iT_{reg}$ s. Effector cells from both young and diabetic  $NOD^{GFP}$  mice upregulated Foxp3 with the same kinetics and produced the same percentage of  $iT_{reg}$ s at the conclusion of culture.

One of the TGF- $\beta$ - and RA-induced genes essential for  $T_{reg}$  development, Foxp3 expression, and contact-dependent suppression is Cx43 (26, 41). This gene is not expressed in naive  $CD4^+$  T cells in steady-state mice, but it is expressed in cells with activated phenotype and in  $T_{reg}$ s, especially  $T_{reg}$  subset expressing low levels of Foxp3.

Cx43 is a major gap junction protein in T lymphocytes, and intercellular transport of cAMP between activated  $T_{reg}$ s and target  $CD4^+$  T cells was shown to inhibit upregulation of CD69, IL-2 gene expression, and cellular proliferation (26). Coculture of target  $CD4^+$  T cells with  $T_{reg}$ s loaded with a fluorescent dye, calcein, demonstrated that inhibition of activation was proportional to the magnitude of calcein transfer and was blocked by gap junction inhibitors. To show that the level of Cx43 expression correlates with gap junction activity, we compared dye transfer between calcein-loaded,  $iT_{reg}$ s, and responder  $CD4^+$  T cells isolated from  $B6^{GFP}$  mice harboring two, one, or no functional alleles of Cx43 gene in  $CD4^+$  T cells (41). To mimic natural interactions between T cells and APCs, we used  $T_{reg}$ s and responder cells expressing transgenic TCR and activated with antigenic peptide presented by bone marrow-derived dendritic cells. Fluorescence of responder cells correlated with Cx43 expression, revealing that gap junction-mediated transport depends on Cx43 expression (Fig. 5B). This result is consistent with a report demonstrating intercellular transport mediated by Cx43 recruited into immunological synapse (42). To further examine Cx43 involvement in  $T_{reg}$  suppression, we have generated  $iT_{reg}$ s from Cx43-sufficient and -deficient  $CD4^+$  T cells.  $iT_{reg}$ -expressing natural levels of Cx43 proved to better inhibit activation of Cx43-sufficient T cells (Fig. 5C). In summary, previously published and current data show how levels of Cx43 regulate intercellular, gap junction-mediated transport and impact  $T_{reg}$ -mediated suppression.

To study how Cx43 could contribute to altered  $T_{reg}$  function, we examined its expression pattern in  $CD4^+$  T cells in young and diabetic NOD mice. Analysis of  $CD4^+$  T cell subsets sorted directly from experimental mice established a baseline for Cx43 expression and revealed low expression in activated and Foxp3 $^{lo}$   $T_{reg}$ s in diabetic  $NOD^{GFP}$  mice (Fig. 5D). Moreover, Cx43 is upregulated to much higher levels only in activated and  $T_{reg}$ s from young, but not diabetic  $NOD^{GFP}$  mice, especially in the presence of TGF- $\beta$  and in the absence of RA (Fig. 5E, 5F).

Age-related changes in the Cx43 expression coincide with the loss of  $T_{reg}$  function and suggest that the  $T_{reg}$  suppression mechanism that relies on generation and intercellular transfer of cAMP might be progressively compromised in aging  $NOD^{GFP}$  mice (7). To further elucidate this mechanism, we compared expression of adenylyl cyclases and phosphodiesterase, enzymes that regulate cAMP levels, in young and diabetic  $NOD^{GFP}$  mice (43). Fig. 6A shows that expression of adenylyl cyclases 4, 7, and 9, major

gated population of  $CD4^+$  Foxp3 $^{GFP-}$  T cells isolated from peripheral (*upper plots*) and pancreatic (*lower plots*) LNs of young (*left panels*) and diabetic (*right panels*)  $NOD^{GFP}$  mice. Flow-cytometry plots show expression of CD44 and CD62L. **(I)** Percentage of activated cells in the gated population of  $CD4^+$  Foxp3 $^{GFP-}$  cells in the peripheral and pancreatic LNs. Individual young mice are represented by squares ( $\square$ ), and triangles ( $\triangle$ ) represent individual aged mice. Mean  $\pm$  SD are shown. **(J)**  $CD4^+$  cells from aged NOD mice have higher proliferative potential. [ $^3$ H]Thymidine uptake of anti-CD3- and anti-CD28-stimulated cells from young (light bar) and diabetic (dark bar) mice is shown. Cells were pulsed at day 3, and proliferation (cpm) was measured after 18 h. Experiment was repeated at least three times. **(K)** Blood glucose level measured in individual young ( $\square$ ) (3–4 wk) and diabetic  $NOD^{GFP}$  mice ( $\triangle$ ) ( $\geq 13$  wk). Glucose levels in aged  $B6^{GFP}$  mice ( $\diamond$ ) are shown for comparison. Asterisks denote statistical significance ( $*p < 0.05$ ).

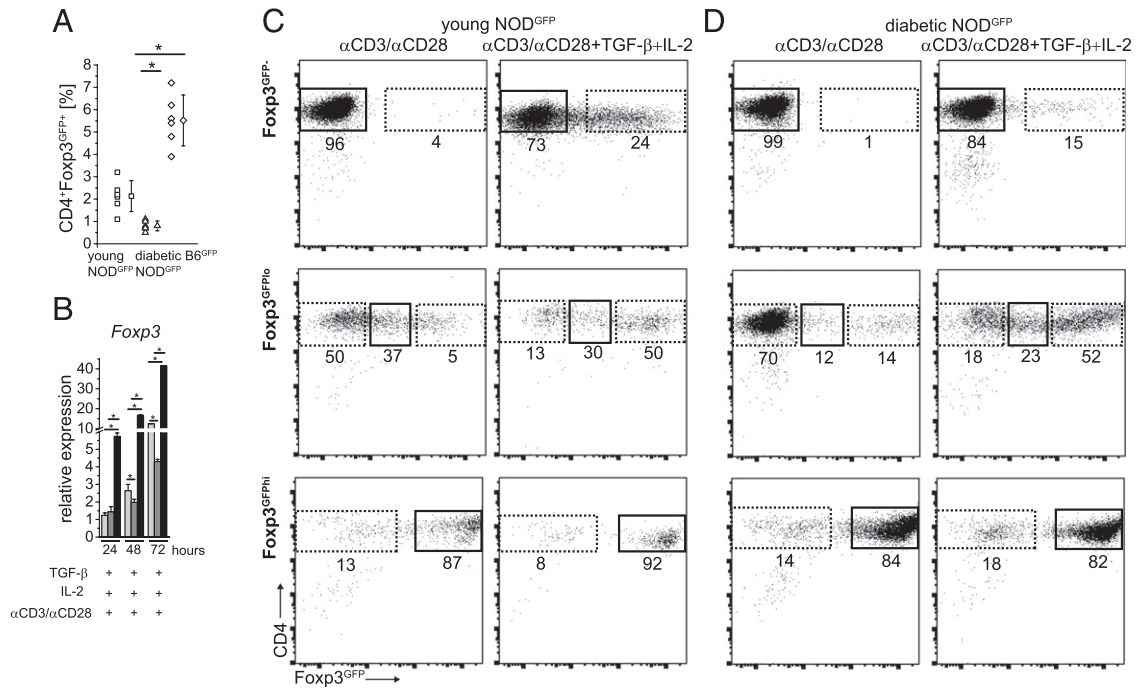


**FIGURE 3.** Stability and kinetics of Foxp3 upregulation in vitro-activated CD4<sup>+</sup> T cells isolated from young and diabetic NOD mice and aged B6 mice. **(A)** The percentage of CD4<sup>+</sup> T cells isolated from peripheral LNs of young (□) and diabetic (△) NOD<sup>GFP</sup> mice and B6<sup>GFP</sup> mice (◇) that upregulate Foxp3 upon activation. Sorted CD4<sup>+</sup>Foxp3<sup>GFP-</sup> cells were activated with plate-bound anti-CD3 and anti-CD28 Abs and analyzed after 3 d. Individual mice are represented by squares, triangles, and diamonds, and mean ± SD are shown for each group of mice. **(B)** Kinetics of Foxp3 upregulation in CD4<sup>+</sup> T cells isolated from young and diabetic NOD<sup>GFP</sup> and B6<sup>GFP</sup> mice. CD4<sup>+</sup>Foxp3<sup>GFP</sup> cells sorted from young (light gray) and diabetic (dark gray) NOD<sup>GFP</sup> and B6<sup>GFP</sup> mice were activated with plate-bound anti-CD3 and anti-CD28 Abs in the presence of IL-2 and TGF-β, and expression of Foxp3 was quantitated with TaqMan probes after 1, 2, or 3 d of a culture. Experiment was repeated two times. **(C and D)** Stability of Foxp3 expression in T<sub>regs</sub> from young (C) and diabetic (D) NOD<sup>GFP</sup> mice. Sorted CD4<sup>+</sup>Foxp3<sup>GFP-</sup> ( $4 \times 10^5$  cells, upper row), Foxp3<sup>GFPlo</sup> ( $2.5 \times 10^5$  cells, middle row), and Foxp3<sup>GFP<sup>hi</sup></sup> ( $2.5 \times 10^5$  cells, lower row) cells from young and diabetic mice were stimulated in vitro with plate-bound anti-CD3 and anti-CD28 Abs in the absence (columns one and three) or in the presence of IL-2 (50 U/ml) and TGF-β (3 ng/ml; columns two and four) and analyzed after 3 d. In vitro-stimulated cells proliferated and their numbers increased  $1.6 \pm 0.4$ ,  $2.3 \pm 0.4$ ,  $1.7 \pm 0.4$ -fold for CD4<sup>+</sup>Foxp3<sup>GFP-</sup>, Foxp3<sup>GFPlo</sup>, and Foxp3<sup>GFP<sup>hi</sup></sup> cells stimulated with anti-CD3 and anti-CD28 in the absence of IL-2 and TGF-β, and increased  $1.9 \pm 0.3$ ,  $3.1 \pm 0.2$ ,  $1.8 \pm 0.1$ -fold for the respective populations stimulated in the presence of cytokines. Gating strategy to isolate Foxp3<sup>GFP-</sup>, Foxp3<sup>GFPlo</sup>, and Foxp3<sup>GFP<sup>hi</sup></sup> cells is shown on Fig. 1C. Rectangles show gates used for sorting (solid lines) and cell populations that upregulated or downregulated Foxp3 expression (broken lines). Numbers denote percentages of cells. Data from one experiment of three is shown. Asterisks denote statistical significance (\* $p < 0.05$ ).

enzymes that increase intracellular cAMP concentration in T lymphocytes, are low in resting T<sub>regs</sub> and are upregulated upon activation in T<sub>regs</sub> isolated from young and diabetic NOD<sup>GFP</sup> mice. Despite lower expression of cyclases in activated T<sub>regs</sub> from diabetic NOD<sup>GFP</sup> mice, especially of adenylyl cyclase 7, all cyclases are significantly upregulated when compared with unstimulated T<sub>regs</sub>. Expression of phosphodiesterase 3b, a major cAMP-degrading enzyme in T<sub>regs</sub>, does not increase in cells from diabetic NOD<sup>GFP</sup> mice upon T<sub>reg</sub> activation (Fig. 6A) (44). Because transcription of the phosphodiesterase gene is downregulated by Foxp3, our data suggest that Foxp3 is still able to control transcription of its target genes even in aging NOD<sup>GFP</sup> mice. Altogether, we conclude that, despite finding dysregulated expression of one adenylyl cyclase, expression of enzymes that control balance between cAMP generation and hydrolysis does not considerably change between young and old NOD<sup>GFP</sup> mice. Thus, low expression of Cx43 in diabetic NOD<sup>GFP</sup> mice likely results in decreased intercellular transport of cAMP, which could contribute to decreased suppressor function of T<sub>regs</sub> in these mice.

To test this hypothesis, we overexpressed Cx43 in expanded T<sub>regs</sub> in vitro. T<sub>regs</sub> expressing higher levels of Cx43 were more efficient in inhibiting proliferation and IFN-γ production than the same cells expressing only low levels of Cx43 (Fig. 6B, 6C). Increased suppression of T<sub>regs</sub> overexpressing Cx43 closely matches and compensates for the reduction of suppression seen between T<sub>regs</sub> isolated from young and diabetic mice. Both inhibition of prolif-

eration and IFN-γ production were abrogated by reagents that restrict intercellular communication through gap junctions, α-glycyrrhetic acid, and connexin extracellular loop mimetic peptide

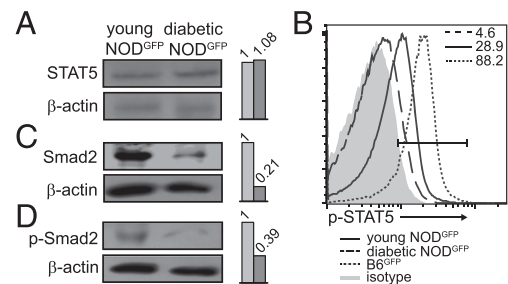


**FIGURE 4.** IL-2 and TGF-β signaling pathways are altered in diabetic NOD<sup>GFP</sup> mice. **(A)** Total STAT5 protein level in total CD4<sup>+</sup> cells isolated from young and diabetic NOD<sup>GFP</sup> mice. **(B)** Phosphorylation of STAT5 was assessed by flow cytometry in total CD4<sup>+</sup> T cells isolated from pancreatic LNs of young (solid line) and diabetic (broken line) NOD<sup>GFP</sup> mice and control B6<sup>GFP</sup> mice (dotted line) stimulated for 15 min in the presence of IL-2 (10 ng/ml). Filled histogram shows staining with isotype-matched Ab. Percentages of positive cells from each mouse are shown. **(C and D)** Expression of Smad2 (C) and its phosphorylated form (D) in young and diabetic NOD<sup>GFP</sup> mice. CD4<sup>+</sup>Foxp3<sup>GFP-</sup> cells sorted from pancreatic LNs were lysed directly or stimulated with TGF-β (1 ng/ml) for 30 min and then lysed in SDS gel-loading buffer. β-Actin was used as a control for equal loading. Bars represent comparison of protein quantities. Experiment was repeated twice.



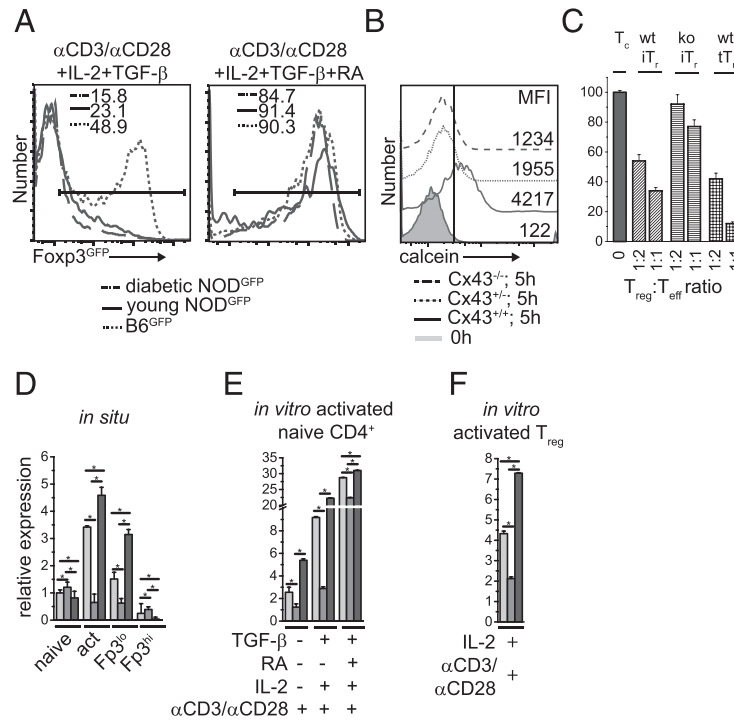


**FIGURE 5.** Decreased suppression of  $T_{reg}$ s in NOD mice is associated with altered expression of Foxp3 and Cx43. **(A)** Coordinated signaling of RA and TGF- $\beta$  enhances the ability of  $CD4^+$  T cells from diabetic NOD mice to upregulate Foxp3 expression in vitro.  $CD4^+$ Foxp3<sup>GFP-</sup> cells sorted from young (solid line) and diabetic (broken line) NOD<sup>GFP</sup> mice and control B6<sup>GFP</sup> mice (dotted line) were stimulated for 3 d with anti-CD3/anti-CD28 Abs in the presence of IL-2 (50 U/ml) and TGF- $\beta$  (3 ng/ml) (left panel) or IL-2, TGF- $\beta$ , and RA (3 nM) (right panel). Representative plots from at least three experiments with three to four mice each are shown. **(B)** Expression levels of Cx43 regulate intercellular communication between iT<sub>reg</sub> and target CD4<sup>+</sup> T cells. Histograms show calcein fluorescence of target CD4<sup>+</sup> T cells expressing two, one, or no functional Cx43 gene alleles. Target CD4<sup>+</sup> T cells were activated with PCC50V54A (0.25  $\mu$ M) antigenic peptide presented by A<sup>b</sup>-expressing bone marrow–derived dendritic cells in the presence of calcein-loaded iT<sub>reg</sub>s. **(C)** Proliferation inhibition assay using Cx43-sufficient responder cells and Cx43-sufficient (diagonal lines) and -deficient (horizontal lines) iT<sub>reg</sub>s and Cx43-sufficient natural T<sub>reg</sub>s (crossed lines). Solid bar represents proliferation of T cells ( $T_c$ ) in the absence of T<sub>reg</sub>s. T<sub>reg</sub> (abbreviated to  $T_r$ ) and responder T cells ( $T_{eff}$ ) were used in a ratio of 1:2 or 1:1. **(D)** Decreased expression of Cx43 in diabetic NOD<sup>GFP</sup> mice. Cx43 expression levels were measured by quantitative PCR in freshly sorted naive ( $CD44^-CD62L^+Foxp3^{GFP-}$ ) and activated ( $CD44^+CD62L^-Foxp3^{GFP-}$ , act) conventional  $CD4^+$  T cells and in T<sub>reg</sub>s expressing low (Fp3<sup>lo</sup>) and high (Fp3<sup>hi</sup>) levels of Foxp3. **(E)** Upregulation of Cx43 expression in sorted naive  $CD4^+$  T cells activated in vitro with plate-bound anti-CD3/anti-CD28 Abs in the presence of IL-2, TGF- $\beta$ , and RA. **(F)** Cx43 expression in sorted  $CD4^+$ Foxp3<sup>GFP+</sup> T<sub>reg</sub>s activated with anti-CD3/anti-CD28 in the presence of IL-2 for 3 d. Representative experiment of three is shown. Quantitative PCR data were obtained with TaqMan probes. Western blot analysis confirmed that Cx43 protein levels in  $CD4^+$  T cell subsets from B6 and NOD mice activated in vitro increased, especially in cells activated in the presence of TGF- $\beta$  (data not shown). Light gray bars in plots (D)–(F) represent cells isolated from young NOD<sup>GFP</sup> mice, gray bars represent cells isolated from diabetic NOD<sup>GFP</sup> mice, and dark gray bars represent cells from B6<sup>GFP</sup> mice.

(Gap26), further demonstrating that overexpression of Cx43 enhances T<sub>reg</sub> function by facilitating contact-dependent suppression (Fig. 6D, 6E) (45, 46). In summary, both cell proliferation and IFN- $\gamma$  production are affected by decreased or increased function of Cx43 in T<sub>reg</sub>s, prompting a possibility that Cx43-dependent mechanisms could be targeted to modulate T<sub>reg</sub> suppression (3, 4).

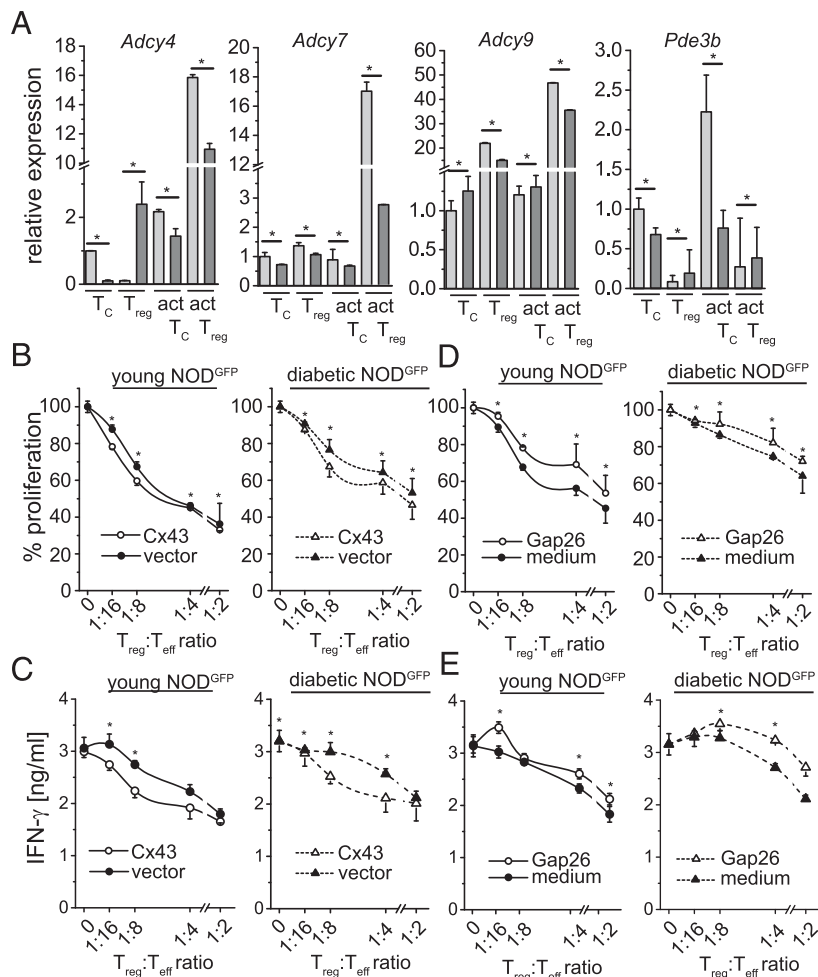
*Redistribution of Cx43 within plasma membrane that promotes gap junction formation and intercellular transport improves suppressor function of T<sub>reg</sub>s in aged NOD mice*

Intercellular communication through gap junctions depends on interaction of two connexons (hemichannels), which are hexamers of Cx43 forming a transmembrane channel, each contributed by the contacting cell (47). Cx43 assembled in gap junctions and in the adjacent domain, called perinexus, is associated with the ZO-1 protein through its C terminus. Disrupting interactions between Cx43 and ZO-1 increased the proportion of connexon hemichannels docked to gap junctions relative to connexons in the perinexus, increased size of gap junction plaques, and facilitated intercellular communication (48). Because ZO-1, as well as Cx43, are expressed in T<sub>reg</sub>s upon activation, interactions between these

two proteins may control the extent of gap junction formation and increase T<sub>reg</sub> suppression. To test this hypothesis, we disrupted interaction between ZO-1 and Cx43 using peptide reagent that mimics C terminus of Cx43 (49). This reagent, called  $\alpha$ CT-1, is engineered to enter cytoplasm and bind the PDZ2 domain of ZO-1, competitively inhibiting its interaction with the C terminus of Cx43. We measured inhibition of proliferation and IFN- $\gamma$  production in the absence and presence of  $\alpha$ CT-1 using responder and T<sub>reg</sub>s isolated from normal B6 mice. As shown in Fig. 7A,  $\alpha$ CT-1 increased intercellular communication between T<sub>reg</sub> and target cells, shown by calcein transport. Addition of  $\alpha$ CT-1 was associated with increased suppressor function of T<sub>reg</sub>s as demonstrated by proliferation inhibition assay and IFN- $\gamma$  production (Fig. 7B). T<sub>reg</sub>s isolated from mice with Cx43 gene deleted in T cells were not affected by presence of  $\alpha$ CT-1 (Fig. 7C). Considering that Cx43 expression is decreased in T<sub>reg</sub>s from diabetic NOD<sup>GFP</sup> mice, we reasoned that suppressor function could be augmented in these cells by increasing proportion of Cx43 available to form gap junctions. In fact, we consistently noticed that  $\alpha$ CT-1 improved suppressor function of T<sub>reg</sub>s isolated from peripheral and pancreatic LNs of young and diabetic NOD<sup>GFP</sup> mice and streptozotocin-treated B6 mice, as demonstrated by inhibition of proliferation and



**FIGURE 6.** Impact of cAMP production and intercellular transport on the suppressor function of T<sub>regs</sub>. **(A)** Expression of adenylyl cyclases (Adcy) 4, 7, and 9 (A) and phosphodiesterase 3b (Pde3b) was measured in freshly isolated conventional CD4<sup>+</sup> Foxp3<sup>GFP</sup> (T<sub>C</sub>) or T<sub>regs</sub> or in the same T cell populations (actT<sub>C</sub> and actT<sub>reg</sub>) activated in vitro. Light gray bars represent cells isolated from young NOD<sup>GFP</sup> mice, and gray bars represent cells from diabetic NOD<sup>GFP</sup> mice. Quantitative PCR was performed using TaqMan assay. Experiment was repeated twice. **(B and C)** Enhanced expression of Cx43 improved tT<sub>reg</sub> suppression. Cx43 was overexpressed in T<sub>regs</sub> sorted from young (○) and diabetic (△) NOD<sup>GFP</sup> mice activated in vitro and used in the proliferation inhibition (B) and IFN-γ production assays (C). Cells transduced with empty vector served as a control (●, ▲). Transduction efficiency exceeded 90% as monitored by the expression of rat CD2 extracellular domain, which was part of the expression vector. **(D and E)** Cx43 mimetic peptide (Gap26) inhibited gap junction formation and decreased suppressor function of T<sub>regs</sub> isolated from young (◆) and aged (▲) NOD<sup>GFP</sup> mice. Proliferation of responder T cells (D) and IFN-γ production (E) was higher in the presence of gap junction inhibitor peptide (Gap26). All experiments were done twice with six repetitions for each measurement. Asterisks denote statistical significance (\**p* < 0.05).



IFN-γ production (Fig. 7D–G, Supplemental Fig. 1C, D). Increased suppression of T<sub>regs</sub> was most apparent when these cells constituted a small fraction of all T cells (5–10%) in the assay, close to the natural proportion of T<sub>regs</sub> in the lymphocyte population. This new reagent enhances gap junction-mediated suppression mechanism, and may allow for compensation of T<sub>reg</sub> deficit without the need to correct the underlying molecular deficit, for example, decreased Cx43 upregulation in diabetic NOD mice. The data presented open a possibility that T<sub>regs</sub>, even in diabetic mice, retain suppressive potential that could be unmasked by treatments that compensate for decreased expression and function of key molecules mediating T<sub>reg</sub> functions.

## Discussion

To better understand molecular processes associated with diabetes development, we examined CD4<sup>+</sup> T cell subsets using a new Foxp3<sup>GFP</sup> reporter mouse, produced on a pure NOD genetic background. This analysis suggests that, similar to C57BL/6 mice, the population of T<sub>regs</sub> in NOD<sup>GFP</sup> mice is heterogeneous with regard to the level and stability of Foxp3 expression (30, 50). Our study extends earlier reports that T<sub>reg</sub> function deteriorates in aged NOD mice and identifies T<sub>regs</sub> expressing low levels of Foxp3 and conventional CD4<sup>+</sup> T cells as cell populations that are mostly affected by age-related dysregulation of Foxp3 expression (22, 51). This is consistent with the recent report that a significant fraction (~20%) of all T<sub>regs</sub> may lose Foxp3 expression (16). Our data suggest that loss and/or downregulation of Foxp3 expression might be caused by impaired signaling by IL-2 and TGF-β as

demonstrated by decreased phosphorylation of STAT5 and Smad2 in aged mice, even in optimal concentration of both cytokines. IL-2 and TGF-β are major cytokines that support peripheral maintenance of tT<sub>regs</sub> and generation of pT<sub>regs</sub> upon antigenic stimulation (34). pT<sub>regs</sub> were specifically identified as suppressor cells protecting NOD mice subject to immunotherapy with anti-CD3 Ab, and their decreased generation in older NOD mice could be regarded as a contributing factor for diabetes development (14). We have previously suggested that continuous upregulation and downregulation of Foxp3 in conventional CD4<sup>+</sup> T cells in response to self-Ags could be an important mechanism of immune tolerance and, based on current data, one could speculate that altered kinetics of this process may impact immunoregulation in NOD mice (30).

The finding that Cx43, a molecule essential for T<sub>reg</sub> suppression and regulated by TGF-β, is only weakly upregulated in activated CD4<sup>+</sup> T cells in NOD<sup>GFP</sup> mice progressing to diabetes complements earlier studies that dysregulation of TGF-β-dependent genes might be an important molecular feature of progression to diabetes (38). Loss- and gain-of-function studies undertaken in this article identify Cx43 as a molecule that directly mediates T<sub>reg</sub> suppression. Moreover, this Cx43 dependence is not regulated by Foxp3, which is consistent with previous reports that functional features and transcriptional signature of T<sub>regs</sub> are controlled by Foxp3-dependent and -independent genes (27, 52). The outcome of decreasing expression of TGF-β-dependent genes in the course of progression to diabetes might be magnified in the case of Cx43 by developing hyperglycemia. Both expression of Cx43 and transport through gap junctions are decreased by hyperglycemia (53, 54). Thus, progression to clinical disease likely combines

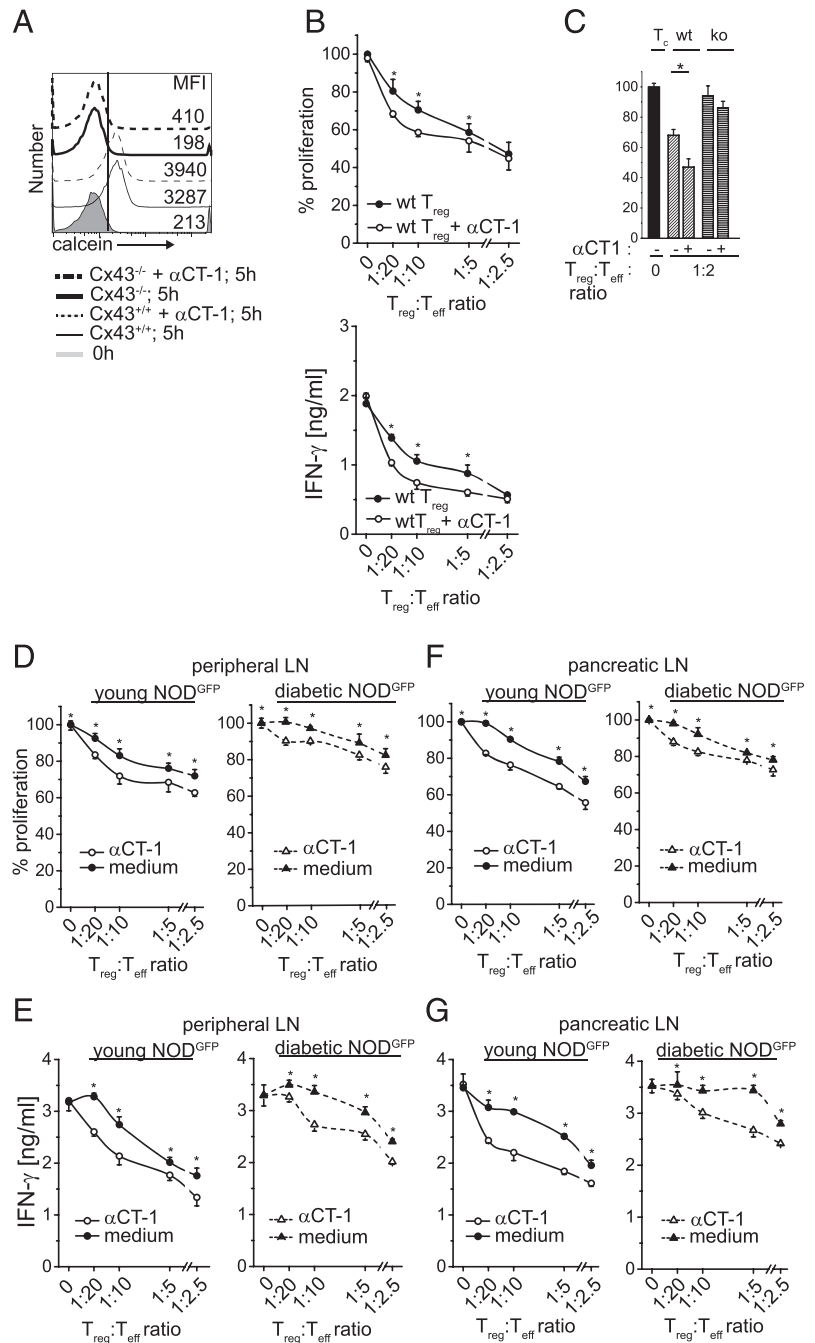


**FIGURE 7.** C-terminal Cx43 mimetic peptide αCT-1 improves T<sub>reg</sub>-mediated suppression. **(A)** αCT-1 increases intercellular communication through gap junctions. Histograms show calcein fluorescence in target Cx43-deficient or -sufficient CD4<sup>+</sup> T cells expressing transgenic receptor activated with antigenic peptide PCC50V54A (0.25 μM) in the presence of bone marrow-derived dendritic cells and calcein-loaded iT<sub>regs</sub> in the presence (dotted lines) or absence (solid lines) of αCT-1. **(B)** Proliferation inhibition and IFN-γ production in the absence and presence of αCT-1. T<sub>regs</sub> and responder cells were isolated from Cx43-sufficient B6 mice. **(C)** αCT-1 does not enhance suppression of T<sub>regs</sub> isolated from B6 mice where Cx43 gene was deleted in T cells. Proliferation inhibition assay in the presence or absence (horizontal lines) of αCT-1. Cx43-sufficient (diagonal lines) and -deficient (horizontal lines) T<sub>regs</sub> were incubated with Cx43-sufficient responder cells in a ratio of 1:2. Due to low proportion of T<sub>regs</sub> in mutant mice, only one ratio of T<sub>reg</sub>/responder cells was tested. Solid bar represents proliferation of responder cells in the absence of T<sub>regs</sub>. **(D–G)** T<sub>regs</sub> isolated from peripheral (D and F) and pancreatic (E and G) LNs of young (○, ●) and aged (△, ▲) NOD<sup>GFP</sup> mice were used in the proliferation inhibition assay (D and E) and to inhibit IFN-γ production (F and G) in the presence (○, △) or absence (●, ▲) of αCT-1. One experiment of two is shown with six repetitions of each well. Asterisks denote statistical differences in cell proliferations between T<sub>regs</sub> cultured in the presence or absence of αCT-1 peptide.

immunological and metabolic factors that form a positive feedback loop and amplify each other.

Expression of Foxp3 and Cx43 is greatly enhanced in activated CD4<sup>+</sup> T cells from aged NOD<sup>GFP</sup> mice by RA, and in vitro generation of iT<sub>regs</sub> is restored to the level seen in young mice. This outcome shows that coordinate signaling, known to use different pathways, is able to compensate for the signal transduction deficit observed in aged cells. In recent reports, RA was shown to inhibit T1D progression, and our data demonstrate that one of the underlying molecular mechanisms of its effect could be to compensate for the age-dependent decline in the ability to upregulate and maintain Foxp3 and Cx43 expression in T<sub>regs</sub> (10, 11). A recent report, however, shows that RA may also decrease specific phosphorylations of Cx43 that lead to increases in intercellular communication through gap junctions revealing complexity of regulatory mechanisms acting directly at the protein level or in-

directly through regulating gene expression (55). This activity of RA is most likely due to directly enhancing association between Cx43 and protein phosphatase 2A, because it does not depend on transcription or new protein synthesis. Altogether, the current and previous reports extend our understanding of how RA regulates T<sub>regs</sub> suppression, especially in the context of diabetes development. It also highlights how interactions between immune system and environmental factors (e.g., diet) may promote or prevent disease progression.

Intercellular communication mediated by gap junctions has been proposed as an important mechanism of T<sub>reg</sub> suppression (7, 26). iT<sub>regs</sub> generated in vitro from CD4<sup>+</sup> T cells isolated from B6 mice that have two, one, or no functional Cx43 gene alleles have progressively lower suppression (41). In this study, by examining Cx43 gene expression pattern in effector cells and T<sub>regs</sub> directly isolated from young (prediabetic) and diabetic mice, or activated

in vitro, we attempted to explain how intercellular communication, mediated by Cx43, may mechanistically contribute to immune regulation of diabetes in NOD mice. We have introduced a novel reagent, the Cx43 mimetic peptide  $\alpha$ CT-1, to promote T<sub>reg</sub>-mediated suppression. Distinct from Gap26, the other mimetic peptide used in this study that inhibits both hemichannels and gap junction channels,  $\alpha$ CT-1 selectively reduces hemichannel activity, whereas promoting gap junction plaque formation (48). This is achieved by a novel mechanism in which  $\alpha$ CT-1 releases undocked hemichannels from ZO-1 PDZ2 tethering at the plaque edge (i.e., the perinexus), prompting them to dock into gap junctions, thereby resulting in a loss of hemichannel activity and a complementary gain of gap junction function. Our results show that  $\alpha$ CT-1 serves as a new experimental tool demonstrating that T<sub>regs</sub>, even in diabetic, hyperglycemic mice, preserve T<sub>reg</sub> suppressor capacity, which can be, at least partially, restored. It is also notable that Cx43 hemichannels have key assignments in the inflammatory response, acting as conduits for the release of pro-inflammatory mediators such as ATP (56). Inhibition of hemichannel activity by promoting gap junction formation thus may represent a further factor to consider in the maintenance of  $\beta$  cells. Dysregulated expression of Cx43 in smooth muscle cells and altered communication through gap junctions were reported in diabetes patients and were considered as a contributing factor in the development of diabetes complications including vascular retinopathy (54, 57). In phase II clinical testing,  $\alpha$ CT-1 improves healing of diabetic foot ulcers and venous leg ulcers—pathologic, slow-healing wounds that are caught in chronic inflammatory states (58). This report shows that Cx43 functions are compromised in T<sub>regs</sub>, directly involved in controlling immunological mechanisms leading to the destruction of pancreatic islets. Exploiting these mechanisms further may lead to a better understanding of immune regulation in diabetes and to the development of new therapies for diabetes and other autoimmune diseases. In conclusion, we hope our report contributes to better understanding of signaling pathways and individual molecules in regulating immune suppression mediated by T<sub>regs</sub> in NOD mice.

## Disclosures

R.G. is an uncompensated member of the scientific advisory board and has modest stock interest (<5% ownership) in FirstString Research Inc., the company that is developing  $\alpha$ CT-1 for indications in skin wound healing. The other authors have no financial conflicts of interest.

## References

- Tisch, R., and H. McDevitt. 1996. Insulin-dependent diabetes mellitus. *Cell* 85: 291–297.
- Yang, Y., and P. Santamaria. 2006. Lessons on autoimmune diabetes from animal models. *Clin. Sci.* 110: 627–639.
- Anderson, M. S., and J. A. Bluestone. 2005. The NOD mouse: a model of immune dysregulation. *Annu. Rev. Immunol.* 23: 447–485.
- Josefowicz, S. Z., L. F. Lu, and A. Y. Rudensky. 2012. Regulatory T cells: mechanisms of differentiation and function. *Annu. Rev. Immunol.* 30: 531–564.
- Sakaguchi, S., T. Yamaguchi, T. Nomura, and M. Ono. 2008. Regulatory T cells and immune tolerance. *Cell* 133: 775–787.
- Kendal, A. R., Y. Chen, F. S. Regateiro, J. Ma, E. Adams, S. P. Cobbold, S. Hori, and H. Waldmann. 2011. Sustained suppression by Foxp3<sup>+</sup> regulatory T cells is vital for infectious transplantation tolerance. *J. Exp. Med.* 208: 2043–2053.
- Bodor, J., T. Bopp, M. Vaeth, M. Klein, E. Serfling, T. Hüning, C. Becker, H. Schild, and E. Schmitt. 2012. Cyclic AMP underpins suppression by regulatory T cells. *Eur. J. Immunol.* 42: 1375–1384.
- Abbas, A. K., C. Benoist, J. A. Bluestone, D. J. Campbell, S. Ghosh, S. Hori, S. Jiang, V. K. Kuchroo, D. Mathis, M. G. Roncarolo, et al. 2013. Regulatory T cells: recommendations to simplify the nomenclature. *Nat. Immunol.* 14: 307–308.
- Belkaid, Y., and G. Oldenhove. 2008. Tuning microenvironments: induction of regulatory T cells by dendritic cells. *Immunity* 29: 362–371.
- Van, Y. H., W. H. Lee, S. Ortiz, M. H. Lee, H. J. Qin, and C. P. Liu. 2009. All-trans retinoic acid inhibits type 1 diabetes by T regulatory (Treg)-dependent suppression of interferon-gamma-producing T-cells without affecting Th17 cells. *Diabetes* 58: 146–155.
- Stosić-Grujčić, S., T. Cvjetičanin, and I. Stojanović. 2009. Retinoids differentially regulate the progression of autoimmune diabetes in three preclinical models in mice. *Mol. Immunol.* 47: 79–86.
- Herman, A. E., G. J. Freeman, D. Mathis, and C. Benoist. 2004. CD4<sup>+</sup>CD25<sup>+</sup> T regulatory cells dependent on ICOS promote regulation of effector cells in the prediabetic lesion. *J. Exp. Med.* 199: 1479–1489.
- Tang, Q., K. J. Henriksen, M. Bi, E. B. Finger, G. Szot, J. Ye, E. L. Masteller, H. McDevitt, M. Bonyhadi, and J. A. Bluestone. 2004. In vitro-expanded antigen-specific regulatory T cells suppress autoimmune diabetes. *J. Exp. Med.* 199: 1455–1465.
- You, S., B. Leforban, C. Garcia, J. F. Bach, J. A. Bluestone, and L. Chatenoud. 2007. Adaptive TGF-beta-dependent regulatory T cells control autoimmune diabetes and are a privileged target of anti-CD3 antibody treatment. *Proc. Natl. Acad. Sci. USA* 104: 6335–6340.
- Chen, Z., A. E. Herman, M. Matos, D. Mathis, and C. Benoist. 2005. Where CD4<sup>+</sup>CD25<sup>+</sup> T reg cells impinge on autoimmune diabetes. *J. Exp. Med.* 202: 1387–1397.
- Zhou, X., S. L. Bailey-Bucktrout, L. T. Jeker, C. Penaranda, M. Martínez-Llordella, M. Ashby, M. Nakayama, W. Rosenthal, and J. A. Bluestone. 2009. Instability of the transcription factor Foxp3 leads to the generation of pathogenic memory T cells in vivo. *Nat. Immunol.* 10: 1000–1007.
- Lundholm, M., V. Motta, A. Löfgren-Burström, N. Duarte, M. L. Bergman, S. Mayans, and D. Holmberg. 2006. Defective induction of CTLA-4 in the NOD mouse is controlled by the NOD allele of Idd3/IL-2 and a novel locus (Ctex) telomeric on chromosome 1. *Diabetes* 55: 538–544.
- voodi-Semiromi, A., M. McDuffie, S. Litherland, and M. Clare-Salzler. 2007. Truncated pStat5B is associated with the Idd4 locus in NOD mice. *Biochem. Biophys. Res. Commun.* 356: 655–661.
- Yamanouchi, J., D. Rainbow, P. Serra, S. Howlett, K. Hunter, V. E. Garner, A. Gonzalez-Munoz, J. Clark, R. Veijola, R. Cubbon, et al. 2007. Interleukin-2 gene variation impairs regulatory T cell function and causes autoimmunity. *Nat. Genet.* 39: 329–337.
- Mellanby, R. J., D. Thomas, J. M. Phillips, and A. Cooke. 2007. Diabetes in non-obese diabetic mice is not associated with quantitative changes in CD4<sup>+</sup>CD25<sup>+</sup>Foxp3<sup>+</sup> regulatory T cells. *Immunology* 121: 15–28.
- Gregori, S., N. Giarratana, S. Smiroldo, and L. Adorini. 2003. Dynamics of pathogenic and suppressor T cells in autoimmune diabetes development. *J. Immunol.* 171: 4040–4047.
- You, S., M. Belghith, S. Cobbold, M. A. Alyanaki, C. Gouarin, S. Barriot, C. Garcia, H. Waldmann, J. F. Bach, and L. Chatenoud. 2005. Autoimmune diabetes onset results from qualitative rather than quantitative age-dependent changes in pathogenic T-cells. *Diabetes* 54: 1415–1422.
- D'Alise, A. M., V. Auyeung, M. Feuerer, J. Nishio, J. Fontenot, C. Benoist, and D. Mathis. 2008. The defect in T-cell regulation in NOD mice is an effect on the T-cell effectors. *Proc. Natl. Acad. Sci. USA* 105: 19857–19862.
- Brusko, T. M., C. H. Wasserfall, M. J. Clare-Salzler, D. A. Schatz, and M. A. Atkinson. 2005. Functional defects and the influence of age on the frequency of CD4<sup>+</sup>CD25<sup>+</sup>T-cells in type 1 diabetes. *Diabetes* 54: 1407–1414.
- Wu, A. J., H. Hua, S. H. Munson, and H. O. McDevitt. 2002. Tumor necrosis factor-alpha regulation of CD4<sup>+</sup>CD25<sup>+</sup>T cell levels in NOD mice. *Proc. Natl. Acad. Sci. USA* 99: 12287–12292.
- Bopp, T., C. Becker, M. Klein, S. Klein-Hessling, A. Palmethofer, E. Serfling, V. Heib, M. Becker, J. Kubach, S. Schmitt, et al. 2007. Cyclic adenosine monophosphate is a key component of regulatory T cell-mediated suppression. *J. Exp. Med.* 204: 1303–1310.
- Kuczma, M., R. Podolsky, N. Garge, D. Daniely, R. Pacholczyk, L. Ignatowicz, and P. Kraj. 2009. Foxp3-deficient regulatory T cells do not revert into conventional effector CD4<sup>+</sup>T cells but constitute a unique cell subset. *J. Immunol.* 183: 3731–3741.
- Ito, M., Y. Kondo, A. Nakatani, and A. Naruse. 1999. New model of progressive non-insulin-dependent diabetes mellitus in mice induced by streptozotocin. *Biol. Pharm. Bull.* 22: 988–989.
- Bayer, A. L., A. Yu, and T. R. Malek. 2007. Function of the IL-2R for thymic and peripheral CD4<sup>+</sup>CD25<sup>+</sup>Foxp3<sup>+</sup>T regulatory cells. *J. Immunol.* 178: 4062–4071.
- Kuczma, M., I. Pawlikowska, M. Kopij, R. Podolsky, G. A. Rempala, and P. Kraj. 2009. TCR repertoire and Foxp3 expression define functionally distinct subsets of CD4<sup>+</sup> regulatory T cells. *J. Immunol.* 183: 3118–3129.
- Pacholczyk, R., H. Ignatowicz, P. Kraj, and L. Ignatowicz. 2006. Origin and T cell receptor diversity of Foxp3<sup>+</sup>CD4<sup>+</sup>CD25<sup>+</sup>T cells. *Immunity* 25: 249–259.
- Kraj, P., R. Pacholczyk, H. Ignatowicz, P. Kisielow, P. Jensen, and L. Ignatowicz. 2001. Positive selection of CD4<sup>(+)</sup>T cells is induced in vivo by agonist and inhibited by antagonist peptides. *J. Exp. Med.* 194: 407–416.
- Davidson, T. S., R. J. DiPaolo, J. Andersson, and E. M. Shevach. 2007. Cutting edge: IL-2 is essential for TGF-beta-mediated induction of Foxp3<sup>+</sup>T regulatory cells. *J. Immunol.* 178: 4022–4026.
- Josefowicz, S. Z., and A. Rudensky. 2009. Control of regulatory T cell lineage commitment and maintenance. *Immunity* 30: 616–625.
- Tang, Q., J. Y. Adams, C. Penaranda, K. Melli, E. Piaggio, E. Sgouroudis, C. A. Piccirillo, B. L. Salomon, and J. A. Bluestone. 2008. Central role of defective interleukin-2 production in the triggering of islet autoimmune destruction. *Immunity* 28: 687–697.
- Murawski, M. R., S. A. Litherland, M. J. Clare-Salzler, and A. Davoodi-Semiromi. 2006. Upregulation of Foxp3 expression in mouse and human Treg is IL-2/STAT5 dependent: implications for the NOD STAT5B mutation in diabetes pathogenesis. *Ann. N. Y. Acad. Sci.* 1079: 198–204.
- Du, W., F. S. Wong, M. O. Li, J. Peng, H. Qi, R. A. Flavell, R. Sherwin, and L. Wen. 2006. TGF-beta signaling is required for the function of insulin-reactive T regulatory cells. *J. Clin. Invest.* 116: 1360–1370.

38. D'Alise, A. M., A. Ergun, J. A. Hill, D. Mathis, and C. Benoist. 2011. A cluster of coregulated genes determines TGF-beta-induced regulatory T-cell (Treg) dysfunction in NOD mice. *Proc. Natl. Acad. Sci. USA* 108: 8737–8742.
39. Vogtenhuber, C., C. Bucher, S. L. Highfill, L. K. Koch, E. Goren, A. Panoskaltis-Mortari, P. A. Taylor, M. A. Farrar, and B. R. Blazar. 2010. Constitutively active Stat5b in CD4+ T cells inhibits graft-versus-host disease lethality associated with increased regulatory T-cell potency and decreased T effector cell responses. *Blood* 116: 466–474.
40. Burchill, M. A., J. Yang, K. B. Vang, J. J. Moon, H. H. Chu, C. W. Lio, A. L. Vegoe, C. S. Hsieh, M. K. Jenkins, and M. A. Farrar. 2008. Linked T cell receptor and cytokine signaling govern the development of the regulatory T cell repertoire. *Immunity* 28: 112–121.
41. Kuczma, M., J. R. Lee, and P. Kraj. 2011. Connexin 43 signaling enhances the generation of Foxp3+ regulatory T cells. *J. Immunol.* 187: 248–257.
42. Mendoza-Naranjo, A., G. Bouma, C. Pereda, M. Ramirez, K. F. Webb, A. Tittarelli, M. N. López, A. M. Kalergis, A. J. Thrasher, D. L. Becker, and F. Salazar-Onfray. 2011. Functional gap junctions accumulate at the immunological synapse and contribute to T cell activation. *J. Immunol.* 187: 3121–3132.
43. Mosenden, R., and K. Taskén. 2011. Cyclic AMP-mediated immune regulation—overview of mechanisms of action in T cells. *Cell. Signal.* 23: 1009–1016.
44. Gavin, M. A., J. P. Rasmussen, J. D. Fontenot, V. Vasta, V. C. Manganiello, J. A. Beavo, and A. Y. Rudensky. 2007. Foxp3-dependent programme of regulatory T-cell differentiation. *Nature* 445: 771–775.
45. Desplantez, T., V. Verma, L. Leybaert, W. H. Evans, and R. Weingart. 2012. Gap26, a connexin mimetic peptide, inhibits currents carried by connexin43 hemichannels and gap junction channels. *Pharmacol. Res.* 65: 546–552.
46. Oviedo-Orta, E., T. Hoy, and W. H. Evans. 2000. Intercellular communication in the immune system: differential expression of connexin40 and 43, and perturbation of gap junction channel functions in peripheral blood and tonsil human lymphocyte subpopulations. *Immunology* 99: 578–590.
47. Maeda, S., and T. Tsukihara. 2011. Structure of the gap junction channel and its implications for its biological functions. *Cell. Mol. Life Sci.* 68: 1115–1129.
48. Rhett, J. M., J. Jourdan, and R. G. Gourdie. 2011. Connexin 43 connexon to gap junction transition is regulated by zonula occludens-1. *Mol. Biol. Cell* 22: 1516–1528.
49. Hunter, A. W., R. J. Barker, C. Zhu, and R. G. Gourdie. 2005. Zonula occludens-1 alters connexin43 gap junction size and organization by influencing channel accretion. *Mol. Biol. Cell* 16: 5686–5698.
50. Komatsu, N., M. E. Mariotti-Ferrandiz, Y. Wang, B. Malissen, H. Waldmann, and S. Hori. 2009. Heterogeneity of natural Foxp3+ T cells: a committed regulatory T-cell lineage and an uncommitted minor population retaining plasticity. *Proc. Natl. Acad. Sci. USA* 106: 1903–1908.
51. Pop, S. M., C. P. Wong, D. A. Culton, S. H. Clarke, and R. Tisch. 2005. Single cell analysis shows decreasing FoxP3 and TGFbeta1 coexpressing CD4+CD25+ regulatory T cells during autoimmune diabetes. *J. Exp. Med.* 201: 1333–1346.
52. Hill, J. A., M. Feuerer, K. Tash, S. Haxhinasto, J. Perez, R. Melamed, D. Mathis, and C. Benoist. 2007. Foxp3 transcription-factor-dependent and -independent regulation of the regulatory T cell transcriptional signature. *Immunity* 27: 786–800.
53. Kuroki, T., T. Inoguchi, F. Umeda, F. Ueda, and H. Nawata. 1998. High glucose induces alteration of gap junction permeability and phosphorylation of connexin-43 in cultured aortic smooth muscle cells. *Diabetes* 47: 931–936.
54. Sato, T., R. Haimovici, R. Kao, A. F. Li, and S. Roy. 2002. Downregulation of connexin 43 expression by high glucose reduces gap junction activity in microvascular endothelial cells. *Diabetes* 51: 1565–1571.
55. Wu, J., R. N. Taylor, and N. Sidell. 2013. Retinoic acid regulates gap junction intercellular communication in human endometrial stromal cells through modulation of the phosphorylation status of connexin 43. *J. Cell. Physiol.* 228: 903–910.
56. Rhett, J. M., S. A. Fann, and M. J. Yost. 2014. Purinergic signaling in early inflammatory events of the foreign body response: modulating extracellular ATP as an enabling technology for engineered implants and tissues. *Tissue Eng. Part B Rev.* 20: 392–402.
57. Zheng, Y. F., D. Z. Dai, and Y. Dai. 2010. NaHS ameliorates diabetic vascular injury by correcting depressed connexin 43 and 40 in the vasculature in streptozotocin-injected rats. *J. Pharm. Pharmacol.* 62: 615–621.
58. Ghatnekar, G. S., C. L. Grek, D. G. Armstrong, S. C. Desai, and R. G. Gourdie. 2015. The effect of a connexin43-based Peptide on the healing of chronic venous leg ulcers: a multicenter, randomized trial. *J. Invest. Dermatol.* 135: 289–298.